UCRL-CONF-233554

LAWRENCE LIVERMORE NATIONAL LABORATORY

RAMP WAVE STRESS-DENSITY MEASUREMENTS OF TA AND W

J. Eggert, M. Bastea, D. Reisman, S. Rothman, J. P. Davis, M. Knudson, D. Hayes, G. Grey, D. Erskine, G. W. Collins

August 9, 2007

Shock Compression of Condensed Matter
Hilo, HI, United States
June 22, 2007 through June 27, 2007

Disclaimer

RAMP WAVE STRESS-DENSITY MEASUREMENTS OF TA AND W

J. Eggert[1], M. Bastea[1], D.B.Reisman[1], S. Rothman[2], J.-P.Davis[3], M.D.Knudson[3], D.B.Hayes[3], G.T.Gray III[4], D. Erskine[1], and G. W. Collins[1]

[1] Lawrence Livermore National Laboratroy, Livermore CA 94551
[2]Atomic Weapons Establishment, Aldermaston, Reading, RG74PR,UK.
[3]Sandia National Laboratory, Albuquerque, NM 87185
[4]Los Alamos National Laboratory, Los Alamos NM 87545

Abstract. Stress-density (σ-ρ) loading paths of both Ta and W under ramped compression were measured up to 300 GPa. For similar ramp loading conditions, σ(ρ) for Ta lies close to the cold curve and significantly below the Hugoniot, while σ(ρ) for W lies close to the Hugoniot and significantly above the cold curve. In both cases, the elastic yield limit is larger than expected from shock-wave experiments on thicker samples. **Keywords:** Ramp wave compression, equation of state, high pressure physics: PACS 64.30.+t, 42.62. b, 61.20.Lc, 62.20.Fe

INTRODUCTION

Much of our understanding of solid-state material response comes from either static or shock compression. Recently-developed ramp-compression techniques now enable shockless compression of solids close to an isentrope to ~ 100 GPa.[1,2,3] In addition to equation-of-state (EOS) information, ramp-wave (RW) compression provides a new way to probe the effects of strain rate on phase transitions, strain hardening, and yield strength since compression times can be tuned from nanoseconds to microseconds[1]. Current RW analysis techniques allow extraction of a continuous sequence of stress-density data under the assumption of self-similarity. These data convolve material effects of both strength and EOS. Previous ramp-wave experiments were limited to stress levels of a few tens of GPa and one report of Al to 240 GPa. This paper reports the highest pressure solid state properties ever for Ta and W. Stress-density (σ–ρ) data for Ta lies close to the cold curve and well below the Hugoniot. For similar loading conditions, σ(ρ) for W is very close to the Hugoniot and is significantly larger than that for the cold curve. In both cases, the elastic-plastic (EP) yield limit is larger than expected from shock wave experiments on thicker samples.

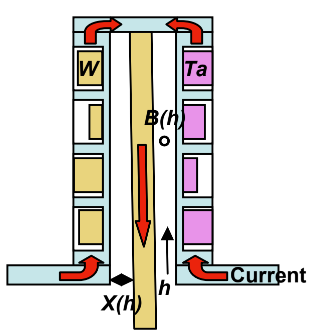

Figure 1. Schematic of target geometry. Because the anode cathode distance is a function of position, x(h), different samples had different drive histories.

EXPERIMENTAL PROCEDURE

The Z accelerator at the Sandia National Laboratories was used to study high-purity Ta[4] and W[5] under RW loading. The RW time was ~ 300ns and the peak stress ~300 GPa. The target, (Fig. 1) was similar to Refs. [2,3]. In all experiments the W-alloy cathode was separated from the Cu anode by a 1 mm vacuum gap. An oxygen-free Cu anode was used for impedance matching of the samples to minimize wave interaction and release effects associated with the panel/sample interface. Four sample disks (OD=6 mm) ~400 to 700 µm thick were glued to the Cu anode. The samples were diamond turned with minimal subsequent polishing for surface-finish enhancement. 300 nm of Ag were evaporated on the polished surface to increase reflectivity for the velocity interferometer (VISAR)[6]. Two fiber- optic bundles, each with four closely packed individual fibers, were pointed one at the center of each sample and one vertically offset by 1.5mm, for light distribution and collection. The free-surface velocity, $u_{fs}(t)$, was monitored on each sample with 2-5 VISAR channels and up to four different sensitivities (0.2962 to 0.848 km/s per fringe) for increased accuracy.

Figure 2 shows resultant free-surface velocity profiles for Ta and W for one experiment. Timing of individual channels was determined to have an accuracy ranging between ~0.5ns and 0.8ns, generally consistent with the temporal spread observed in the individual traces. In general the error in velocity attributable to the measurement of the Doppler shift is ~2% of the sensitivity setting[6]. Extensive two-dimensional magneto-hydrodynamic simulations show that for an ideal geometry the pressure is uniform at all times to < 1% over the central 3mm of each sample. This was also supported experimentally.

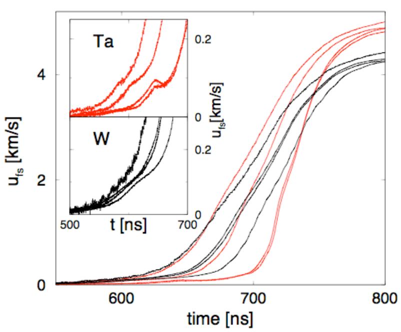

Figure 2. Measured wave profiles for experiment Z1683. Also shown in the insets are a magnified section of the elastic precursor. Red (black) lines are Ta (W).

While the pressure uniformity appears good in the central region of each sample, the sample-to-sample pressure histories are different. This is shown in Fig. 2, where for samples with the same thickness at the top and bottom of the anode (Fig. 1), there is an offset in the free surface velocity, U_{fs}, which suggests variations of the loading paths between samples. This may arise from a non-parallel anode-cathode assembly. Since, $P \sim B^2 \sim x^2$, for $\Delta P/P \sim 1\%$ pressure variation from the top sample to the bottom sample, the anode cathode distance, x, needs to be constant within ~ 5 µm over the 26 mm distance spanning the samples. This is an engineering challenge. Fig. 3 shows the stress density attained for several experiments assuming the drive pressure (and thus x) was the same for each sample on a given panel. These results used the iterative analysis techniques of Rothman et al.,[7] however similar results are attained using the backwards-integration technique of Hayes et al.[2]

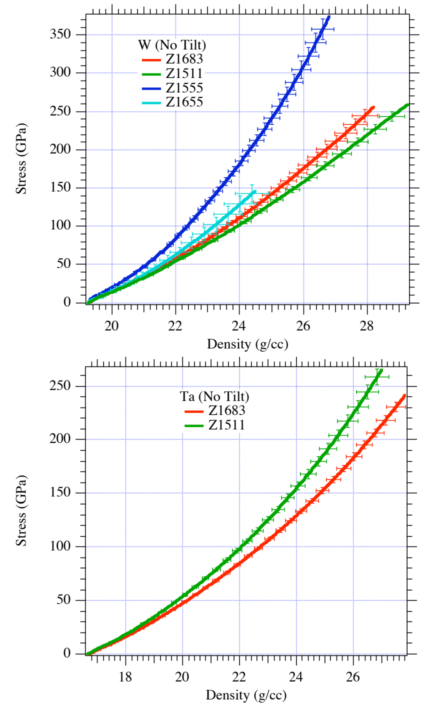

Figure 3. Calculated stress-density for all experiments on W and Ta assuming the pressure drive on all samples is the same.

Simulations show that a simple scaling of the pressure at each panel by 1% leads to variations in the EOS comparable to those shown in Fig. 3. Since this level of tilt could not be ruled out by the target assembly procedures, and because variations are opposite on opposite panels, cathode tilt is the lead candidate for causing the observed lack of shot-to-shot reproducibility. This drive non-uniformity violates the fundamental assumption used in all previous ramp-wave analyses, that the pressure drive is identical for all sample thicknesses.

To obtain self consistency between the different experiments a new analysis procedure was developed to approximately account for tilt in the anode-cathode assembly. The primary assumption for this analysis is that since the drive current, $I(t)$, is identical for each panel, the pressure drive, $P_i(t)$, can be scaled linearly (small-tilt approximation) by the cathode tilt. This first-order correction to the data does not account for time-dependent geometry or higher order distortions.

We modified the iterative analysis developed by Rothman and Maw[7] and Smith et al[1] to account for cathode tilt by scaling the pressure drive. Standard iterative analysis consists of: A) Assume an EOS in the form of a Lagrangian sound speed as a function of particle velocity, $C_L(Up)$. B) Solve the backward problem for each step to find the pressure drive for each free-surface wave profile. C) Propagate each pressure drive forward using the same assumed EOS to obtain the in-situ velocity profiles that would occur at each measurement location for semi-infinite samples. D) Assuming identical pressure drives for each sample, a linear fit through the time , *t(Up)*, versus sample thickness for the corrected wave profiles is used to find a new estimate of $C_L(Up)$. Steps B-D are then iterated to convergence of $C_L(Up)$ which can then be integrated to obtain the stress-density relation.

If the pressure-drive for sample i can be written as, $P_i(t)=\left[1+s_i(t)\right]p(t)$, the iterative procedure can be modified using this scaling in step C before the forward propagation. The modified iterative procedure then generates a $C_L(Up)$, and a benchmark pressure drive $p(t)$, for any assumed $s_i(t)$. The simple assumption of linear pressure scaling discussed above takes the form, $s_i(t)=\varepsilon i$ where ε controls the tilt magnitude. For all of the results reported here ε was sufficiently small that convergence was not an issue.

After extensive analysis, it was found that by comparing the measured wave profiles with those predicted by the modified iterative procedure, an optimum value of ε could be determined for several different sample geometries. When the sample thicknesses were arranged monotonically from top to bottom, a unique solution was not found unless the same geometry was used on both panels. When the sample thicknesses were not

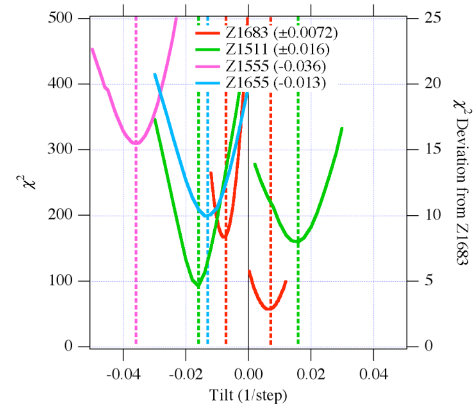

Figure 4. Quality of fit for all experiments with Ta and W. For Z1683, χ^2 is the difference between the calculated and measured wave profiles normalized by uncertainties in Ufs and time (right axis). Other experiments are defined as the deviation from z1683

monotonic with position a unique solution is found and ε is determined. One shot, Z1683, had such a geometry (as shown in Fig. 1) with approximate sample thicknesses of 590/490/690/590 μm for W and 710/560/460/710 μm for Ta . A figure of merit, $\chi^2 \propto \sum\left[\left(\frac{\partial U_{fs}}{\partial t}\Delta t\right)^2+\Delta U_{fs}^2\right]$, was defined by how closely the predicted and measured wave profiles agreed and is shown as a function of ε in Fig. 4 (red curves). Note that since the W and Ta where on opposite sides of the tilted cathode, the resultant values for ε should obey the constraint $\varepsilon_W=-\varepsilon_{Ta}$. The independently determined ε_W and ε_{Ta} do indeed fulfill this constraint. We have made this constraint explicit in our determination of the EOS for this shot as shown by the dashed lines at $\varepsilon_{Z1683}=\pm 0.0072$ in Fig. 4.

Another experiment, Z1511 had W and Ta mounted on opposite sides of the cathode, but with samples arranged from thickest to thinnest on both sides. In that case, as in the analysis of Z1683, $\varepsilon_W=-\varepsilon_{Ta}$ should hold. We tested this constraint by varying each ε to get the best agreement, with the $C_L(Up)$ of Z1683, $\chi^2_{Z1683}\propto\sum\left[C_L\left(U_{fs}\right)-C_L^{Z1683}\left(U_{fs}\right)\right]^2$, as shown in Fig. 4 (green curves). Again, independent determinations of ε_W and ε_{Ta} are nearly equal in magnitude, and we made use of this explicitly in our determination of the EOS for this shot as shown by the dashed lines at $\varepsilon_{Z1511} = \pm 0.016$ in the figure. This is strong evidence that our simple corrections for tilt are effective. Finally, for two other experiments on W we could only obtain ε_W by requiring agreement with the $C_L(Up)$ of Z1683. These results are also shown in Fig.4, $\varepsilon_{Z1555} = -0.036$, $\varepsilon_{Z1655} = -0.013$.

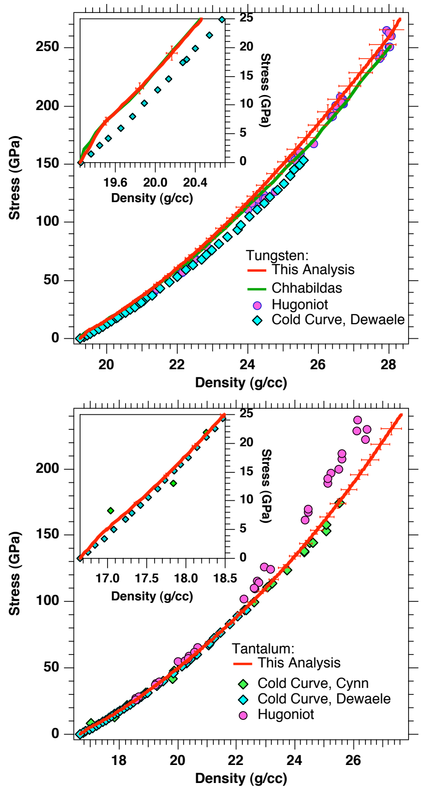

Figure 5. Ramp compression stress density data for W and Ta with Hugoniot[8] and cold curve[9] data.

RESULTS AND DISCUSSION

The final determinations for $C_L(Up)$ from all of the experiments (4 for W, and 2 for Ta) were averaged and integrated to find our final determination of stress and density, Figure 4 shows the results compared to Hugoniot[8] and cold curve data[9]. Uncertainties shown are those determined for shot Z1683 using uncertainties in U_{fs} (0.003 km/s), time (0.8 ns), and step height (including floor and glue-bond, 3 μm). The shot-to-shot spread in the data is less than the uncertainties shown. Also shown for W are ramp compression data (actually a series of small shocks) from Chhabildas who used graded density impactors with ramp compression times of microseconds. Our data show the stress in W is comparable to the W Hugoniot and previous data from Chhabildas[10], and much higher than the cold curve. The stress for ramp compressed Ta under the same conditions is much lower than the Ta Hugoniot and quite close to the cold curve[9]. The insets in Fig. 5 show a magnified region near the elastic-plastic region. This reveals that much of the difference between the ramp compression and cold curve stress-density is due to the elastic-plastic precursor.

ACKNOWLEDGEMENTS

We thank Tim Uphaus for overseeing the preparation and assembly of samples. This work was performed under the auspices of the U.S. Department of Energy by University of California, Lawrence Livermore National Laboratory under Contract W-7405-Eng-48.

REFERENCES

1. D.B.Reisman et al. J. Appl. Phys. 89 1625 (2001). C. Hall et al. Rev. Sci. Instrum. 72 3587 (2001). R. Smith et al. PRL 98, 065701(2007).
2. D.Hayes et al., J. Appl. Phys. **96** 5520 (2004).
3. JP.Davis, J. Appl. Phys. **99** 103512 (2006).
4. G.T.Gray III et al., J.Appl.Phys. **94** 6430 (2003) and refs. therein.
5. W samples were commercially pure, fabricated via powder metallurgy, received as a fully annealed 12.5-mm thick plate, with grain size nominally 20 microns.
6. Hemsing, Rev. Sci. Instr. **50** 73(1979). D.H. Dolan, Sandia Report, SAND2006-1950 (2006).
7. S. Rothman et al., J. Phys. D-Appl. Phys., 38 733 (2005).
8. A. C. Mitchell, W. J. Nellis, J. Appl. Phys. 52, 3363(1981). S.P.Marsh, LASL Shock Hugoniot Data (University of California Press, Berkeley, 1980). R.F.Trunin et al, Experimental data on Shock compression and Adiabatic Expansion of Condensed Matter. (Sorov, VNIIEF, 2001).
9. A. Dewaele, P. Loubeyre, Phys.Rev.B 72 134106(2005). S.T.Weir et al, Phys. Rev. B 58 11258(1998). H. Cynn, C.S.Yoo, Phys. Rev. B 59, 8526 (1999).
10. L.C. Chhabildas, et al. Sandia Report, SAND88-0306 (1988).